Diastereoisomerism and electrochemical behaviour— an investigation of redox-active cyclophanes

Michael B. Leitner,[a] Thomas Kreher,[b] Helmut Sonnenschein,*[,b] Burkhard Costisella[c] and Jürgen Springer[a]

[a] *Technische Universität Berlin, Institut für Technische Chemie, Fachgebiet Makromolekulare Chemie, Straße des 17. Juni 124, D-10623 Berlin, Germany*
[b] *Institut für Angewandte Chemie Berlin-Adlershof, Abteilung Organische Synthese, Rudower Chaussee 5, D-12484 Berlin, Germany*
[c] *Institut für Angewandte Chemie Berlin-Adlershof, Abteilung Analytik, Rudower Chaussee 5, D-12484 Berlin, Germany*

The influence of diastereoisomerism on the electrochemical behaviour of the atropisomeric cyclophanes 1a and 1b was found by cyclovoltammetric studies. Compound 1a can be oxidized and reduced reversibly in a two step redox process similar to that of model compound 2. In contrast, 1b shows a different electrochemistry. As a result of a detailed investigation of 1b a complex reaction scheme can be postulated starting with a chemical reaction after the first oxidation step. The special spatial situation in 1b makes possible this EC mechanism reaction, which does not occur in 1a or in unbridged biindolizines.

Introduction

Recently, we reported the synthesis of diastereomers of redox active cyclophanes.[1] We used as electroactive unit 3,3′-biindolizine known as a reversible two step redox system.[2–5] The synthesized macrocycles contain three independent elements of chirality as a result of the ansa-chirality of cyclophanes and the atropisomerism of the 3,3′-biindolizines. It was possible to isolate pure diastereomers of the macrocycles. In one case both pairs of enantiomers (**1a** and **1b**) were characterized by X-ray analysis.

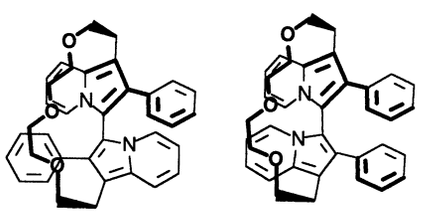

1a **1b**

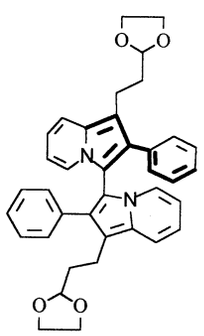

2

The spatial situation in the two isomers **1a** and **1b** is completely different due to axial chirality. In diastereomer **1a** the two heterocyclic systems are located on opposite sides of the ether bridge (*E*-form) and in **1b** both of them are on the same one (*Z*-form). It has been shown that the cyclic voltammograms of **1a** had two redox waves, whereas **1b** gave three redox waves. Evidently, a relation between the diastereoisomerism and the electrochemical behaviour exists.

In the present paper we describe a detailed investigation of this electrochemical phenomenon. As an unbridged model compound we synthesized the new biindolizine **2** and compared its voltammetric behaviour with the data of **1a** and **1b**.

Results and discussion

The new redoxactive 3,3′-biindolizine **2** was synthesized as a model compound with two 2-ethyl-1,3-dioxolanes as ether-like functions by a reaction sequence, which has been described previously (Scheme 1).[1]

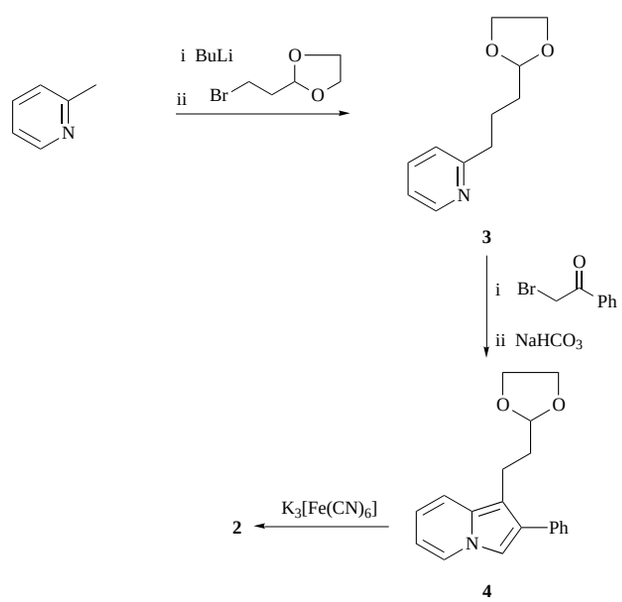

Scheme 1 Reaction sequence leading to **2**

Such substituted 3,3′-biindolizines can be oxidized and reduced reversibly in a two step redox process according to the general reaction scheme shown in Scheme 2.[3,6] In the first oxidation step (**1**) the biindolizine **5** is oxidized reversibly by a

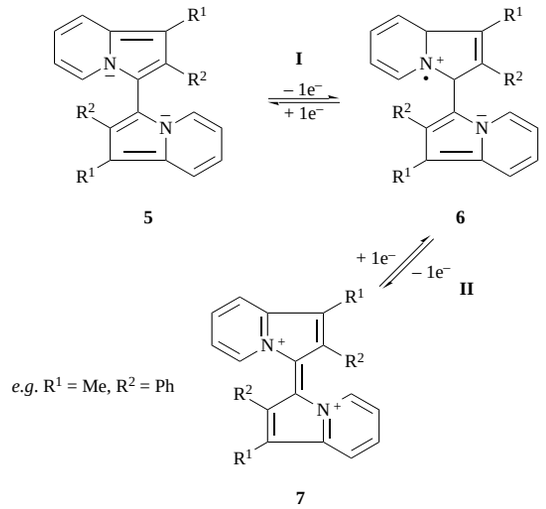

5 6 7

Scheme 2 General reaction scheme for the reversible two step redox reaction of substitued biindolizines

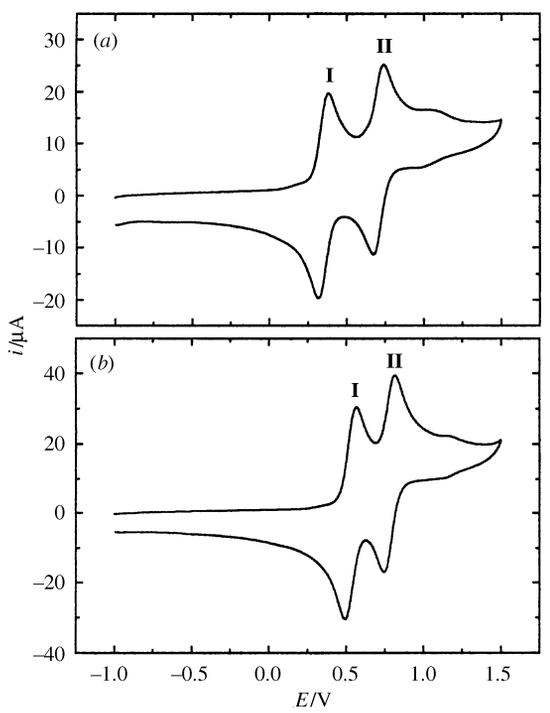

Fig. 1 Cyclic voltammograms of **1a** (*a*) and **2** (*b*) sweeping with $v = 0.4$ V s^{-1}

one electron transfer forming the radical cation **6**. In the second single electron transfer process (**II**) the radical cation **6** is transformed reversibly to the dication **7**.

The compounds **1a**, **1b** and **2** were studied by cyclic voltammetry using 0.1 mol dm^{-3} tetrabutylammonium hexafluorophosphate (Bu_4NPF_6) in acetonitrile as electrolytic solvent. The formal potentials $E^{0'}$ of the redox waves that appeared were obtained by averaging the cathodic and anodic peak potentials: $E^{0'} = (E_{pc} + E_{pa})/2$.[7] The peak potentials E_{pa} and E_{pc} were determined by the method of Nicholson.[8] The separation of the peak potentials ΔE_p was calculated: $\Delta E_p = E_{pa} - E_{pc}$. The anodic peak currents i_{pa} were determined with respect to the blank as has been described before.[9] In cyclic voltammetric measurements the sweep rate v is a useful parameter to analyse redox systems.[7,8] We used five sweep rates in the range $v = 0.02$–10 V s^{-1}. As shown in Fig. 1 the cyclic voltammograms of **1a** and **2** were similar and showed two reversible redox waves with the corresponding formal potentials at $E^{0'}$**I** = 0.350 V (**1a**),

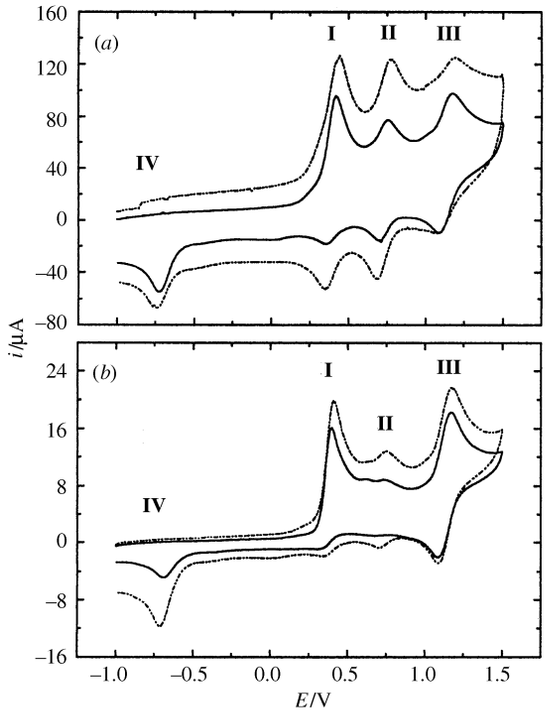

Fig. 2 Cyclic voltammograms of **1b** sweeping with $v = 10$ V s^{-1} (*a*, broken line), $v = 2$ V s^{-1} (*a*, solid line, scaled up by a factor of 2.0), $v = 0.4$ V s^{-1} (*b*, broken line) and $v = 0.08$ V s^{-1} (*b*, solid line, scaled up by a factor of 1.8)

$E^{0'}$**I** = 0.527 V (**2**) for the first redox wave (**I**) and $E^{0'}$**II** = 0.706 V (**1a**), $E^{0'}$**II** = 0.780 V (**2**) for the second redox wave (**II**) *vs.* the Ag/AgCl electrode as reference (Table 1, $v = 0.4$ V s^{-1}). Additionally, a very small third redox wave was detected at *ca.* 1 V. The observed differences of the $E^{0'}$ and $\Delta E^{0'}$ values for the compounds **1a** and **2** are on the same scale as already described for different substituted biindolizines.[3]

The variation of the sweep rate v had no effect on both $E^{0'}$**I** and $E^{0'}$**II** and consequently on $\Delta E^{0'}$ values. The ΔE_p values were 60–105 mV for **1a** and 57–132 mV for **2** respectively. The deviations from the theoretically expected value of 59 n mV for a reversible redox reaction are explained by distortions due to solution resistance effects and electronic smoothing of data.[7,8]

In contrast, the cyclic voltammograms of **1b** were more complex depending on the sweep rate. As shown in Fig. 2(*a*) three redox waves (**I**, **II**, **III**) and an additional cathodic peak (**IV**) were obtained on sweeping with high rates ($v = 2$ and $v =$ 10 V s^{-1}). The redox pattern changed remarkably using lower sweep rates [Fig. 2(*b*), $v = 0.4$ and $v = 0.08$ V s^{-1}].

At $v = 0.4$ V s^{-1} the oxidation peak **II** was decreased dramatically in relation to the oxidation peaks **I** and **III**. Simultaneously, the reduction peaks **I** and **II** were decreased in relation to the reduction peaks **III** and **IV**. At $v = 0.08$ V s^{-1} the oxidation peak **II** and the reduction peaks **I** and **II** disappeared. The measured formal potentials at $v = 0.4$ V s^{-1} were $E^{0'}$**I** = 0.372 V, $E^{0'}$**II** = 0.729 V, $E^{0'}$**III** = 1.130 V and the reduction peak **IV** appeared at E_{pc}**IV** = −0.709 V (Table 2).

Since the $E^{0'}$ values of **1b** for the waves **I** and **II** were similar to those of **1a**, it could be concluded that both redox processes **I** and **II** were the same for **1a** and **1b** in accordance to the general reaction scheme (Scheme 2).† We expect the decrease of the redox waves to be a result of a chemical reaction during redox cycling of **1b**. To confirm this, the redox waves **I** and **II** were investigated as a function of the sweep rate ($v = 0.1$–10 V s^{-1}). As shown in Fig. 3(*a*) the oxidation peak **II** and the reduction

† As we have described before, a very small third oxidation wave (**III**) was also observed in the case of **1a** and **2**. But only the cyclic voltammograms of **1b** show a significant change in the redox pattern.

Table 1 Cyclovoltammetric data of **1a** and **2** scanning with five different sweep rates

Compound (conc./mmol dm^{-3})	v/V s^{-1}	$E^{0'}$**I**/V	$E^{0'}$**II**/V	$\Delta E^{0'}$/V	ΔE_p**I**/mV	ΔE_p**II**/mV	i_{pa}**I**/μA	i_{pa}**II**/μA
1a (0.55)	10.098	0.351	0.706	0.355	104	105	130.9	151.9
	2.002	0.347	0.706	0.359	74	77	49.7	60.2
	0.400	0.350	0.706	0.357	63	66	19.8	25.2
	0.080	0.346	0.703	0.357	60	60	8.5	11.2
	0.020	0.349	0.703	0.355	65	60	4.3	6.1
2 (0.51)	10.248	0.524	0.788	0.264	132	132	180.2	215.8
	2.002	0.529	0.783	0.254	91	93	73.0	90.8
	0.400	0.527	0.780	0.253	72	71	30.6	39.6
	0.080	0.526	0.780	0.255	69	66	13.3	17.7
	0.020	0.527	0.776	0.249	72	57	6.7	9.1

Table 2 Cyclovoltammetric data of **1b** (c: 0.55 mmol dm^{-3}) scanning with five different sweep rates

v/V s^{-1}	$E^{0'}$**I**/V	$E^{0'}$**II**/V	$E^{0'}$**III**/V	E_{pc}**IV**/V	ΔE_p**I**/mV	ΔE_p**II**/mV	ΔE_p**III**/mV	i_{pa}**I**/μA	i_{pa}**II**/μA	i_{pa}**III**/μA
10.098	0.394	0.728	1.136	−0.747	90	87	101	127.0	124.5	125.0
2.002	0.387	0.732	1.123	−0.725	60	41	94	48.1	38.8	49.1
0.400	0.372	0.729	1.130	−0.709	74	52	90	20.0	12.8	21.8
0.080	*a*	0.739	1.125	−0.706	*a*	34	79	9.0	5.0	10.2
0.020	*a*	*a*	1.120	−0.673	*a*	*a*	82	4.6	2.9	6.0

[a] No value because the cathodic peak was not detected.

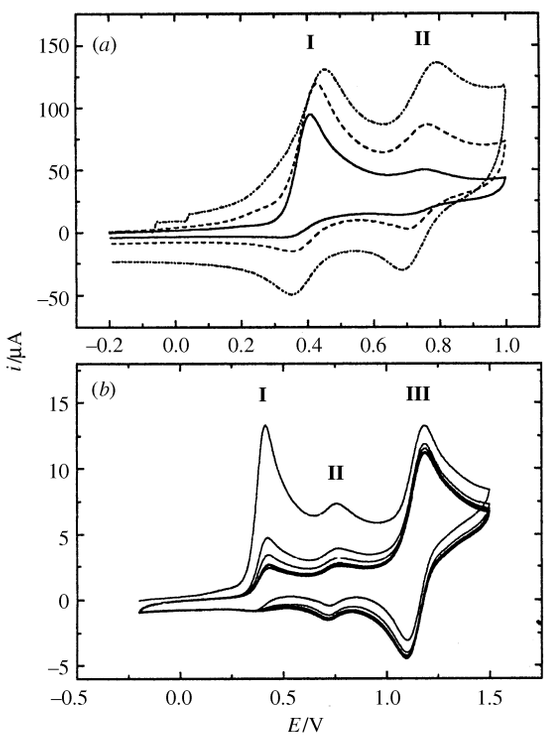

Fig. 3 Cyclic voltammograms of **1b**: (*a*) the redox waves **I** and **II** sweeping with $v = 10$ V s^{-1} (dotted line), $v = 1$ V s^{-1} (dashed line) and $v = 0.1$ V s^{-1} (solid line); (*b*) multisweep experiment of the redox waves **I-III** sweeping with $v = 0.16$ V s^{-1} six scans without a delay

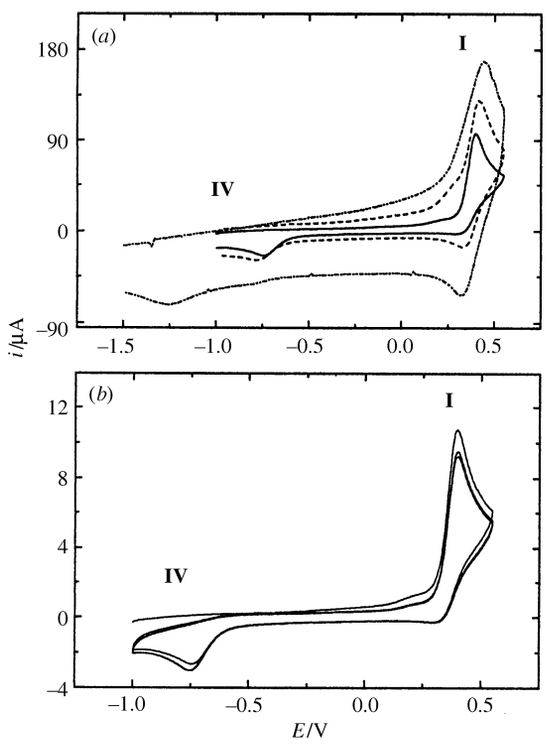

Fig. 4 Cyclic voltammograms of the redox wave **I** and the reduction peak **IV** of **1b**: (*a*) sweeping with $v = 10$ V s^{-1} (dotted line), $v = 1$ V s^{-1} (dash line) and $v = 0.1$ V s^{-1} (solid line); (*b*) multisweep experiment sweeping with $v = 0.1$ V s^{-1} three scans without a delay

peaks **I** and **II** were strongly diminished at $v = 0.1$ V s^{-1} in comparison to higher sweep rates, which indicated clearly the appearance of a chemical reaction following the oxidation reaction **I**.

Fig. 2 indicates that the product of this chemical reaction could be oxidized reversibly at the redox wave **III**. To prove this, a multisweep experiment with no time delay was carried out for the redox waves **I–III** of **1b** [Fig. 3(*b*)] using a low sweep rate due to the timescale of the chemical reaction ($v = 0.16$ V s^{-1}). The redox wave **I** declined strongly during the multisweep cycling, which could be explained by the fact that compound **5** decreased due to the chemical reaction of **6** forming a new species. The oxidation peak **III** reaches, in the first scan, the height of the oxidation peak **I**, which is a strong indication for the nearly complete chemical reaction of **6**. The redox wave **III** showed only a small decay between the first and second scan and no further decay in subsequent scans, which is typical for the multisweep cycling of reversible redox systems. Therefore, this new species was oxidized and reduced reversibly in wave **III**.

As shown in Fig. 4(*a*) the relationship between the redox wave **I** and the reduction peak **IV** was studied as a function of the sweep rate. Sweeping with $v = 10$ V s^{-1} the reduction peak **I** occurred clearly, but the reduction peak **IV** appeared weakly at the potential of −1.25 V. Sweeping with $v = 0.1$ V s^{-1} the reduction peak **I** was not detected, but the reduction peak **IV** appeared at the potential of −0.7 V. Therefore, the product of

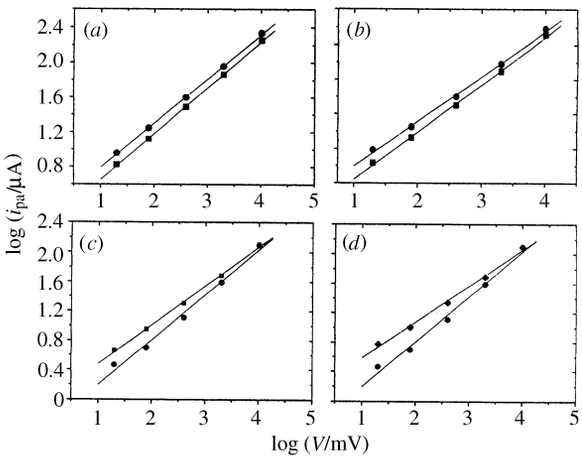

Fig. 5 Linear regression plots of log i_{pa} *vs*. log *v* for the oxidation waves **I**-**III** (Tables 1 and 2): (*a*) **1a** (**I**: squares, **II**: circles); (*b*) **2** (**I**: squares, **II**: circles); (*c*) **1b** (**I**: squares, **II**: circles); (*d*) **1b** (**II**: circles, **III**: diamonds)

the chemical reaction of **6** could be reduced, too, which was not linked with the appearance of the redox wave **III**. It was proved in an additional experiment that **1b** could not be reduced directly in the potential range mentioned. As shown in Fig. 4(*b*) a multisweep experiment was carried out sweeping with $v = 0.1$ V s^{-1}. The oxidation peak **I** showed no significant decay, which was different to the multisweep experiment in Fig. 3(*b*). This fact could be explained by a chemical reaction leading to **1b** again. An oxidation peak corresponding to the reduction peak **IV** was not observed.

The variation of the sweep rate *v* had no effect on the $E^{0'}$ values of **1b** (Table 2). Only the value of E_{pc}**IV** had a significant shift to less cathodic potential using a lower sweep rate (Table 2, $v = 10$ V s^{-1} : E_{pc}**IV** = −0.747 V, $v = 0.02$ V s^{-1} : E_{pc}**IV** = −0.673 V). The observed shift of 74 mV could be explained by the fact that the reduction wave **IV** was irreversible. The ΔE_p values for the redox waves **I**–**III** of **1b** were in the range 34–101 mV, which was in good agreement with the theory of reversible electron transfer.[7,8]

Processes featuring adsorption had to be distinguished from purely diffusion controlled reversible redox processes. Therefore, the anodic peak currents i_{pa} were measured as a function of the sweep rate *v* (Tables 1 and 2). A plot of 10 g i_{pa} *vs*. 10 g *v* is linear with the slope *a* of 0.5 for a diffusion peak ($i_{pa} \sim v^{\frac{1}{2}}$) and the slope *a* of 1.0 for an adsorption peak ($i_{pa} \sim v$).[7,8] The corresponding plots are given in Fig. 5.

For **1a** and **2** the slope *a* was *ca*. 0.5 for the oxidation waves **I** and **II** (Table 3). It was concluded that **1a** and **2** can be oxidized and reduced reversibly in a diffusion controlled two step process according to Scheme 2. For **1b** the slope *a* was *ca*. 0.5 for the oxidation waves **I** and **III** and *ca*. 0.6 for the oxidation wave **II** (Table 3). The deviation of *a* for **II** from 0.5 was explained by the chemical reaction appearing after the oxidation step **I**.

Due to the results of our cyclic voltammetric studies the general reaction scheme in Scheme 2 had to be modified for **1b** yielding the scheme shown in Scheme 3.

In **1b**, the spatial distance between the two indolizine units is small due to the fact that the bridge hinders their free rotation in sectors of 90°. So the radical cation **8** obtained in the oxidation process **I** is enabled to attack the second indolizine system forming a single bond between positions 5 and 5′ in **10**, which is shown in Scheme 3. The oxidation step **III** produces the dication **12** with an additional single bond instead of a double bond between 3 and 3′ in oxidized unbridged biindolizines. Reduction of the whole system leads again to the radical cation **10**. In the reduction step **IV** the corresponding neutral compound **11** is formed. We expect **11** to be a compound with a high steric tension (especially as a result of the double bond between 3 and 3′), capable of undergoing a pericyclic ring-opening reaction

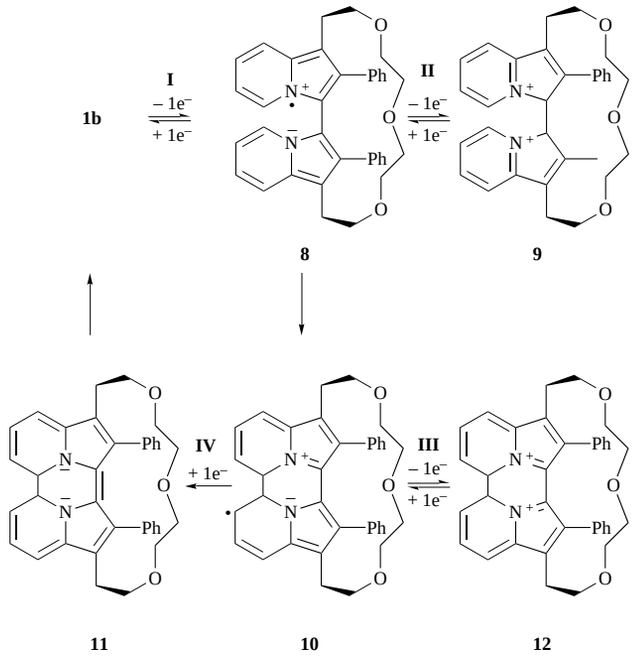

Scheme 3 Reaction scheme for **1b**

Table 3 The exponent value *a* of the oxidation waves **I**–**III** calculated by linear regression of the plot of log $i_{pa} = a$ log v + log K for **1a**, **1b** and **2**

Compound	*a***I**	*a***II**	*a***III**
1a	0.55 ± 0.01	0.52 ± 0.01	*a*
1b	0.53 ± 0.01	0.61 ± 0.04	0.49 ± 0.02
2	0.53 ± 0.01	0.51 ± 0.01	*a*

[a] No peak.

giving the starting material **1b** again. This chemical reaction of **11** may explain the absence of an oxidation peak corresponding to the reduction wave **IV**.

The rigidity of the bridged compounds **1a** and **1b** is different to that of the unbridged compound **2**. Therefore, distinguishable diffusion coefficients should be expected. The diffusion coefficients D_o were calculated by the expression $i_p = 0.4463nFAC_o(nFvD_o/RT)^{\frac{1}{2}}$ for reversible, diffusion controlled electron transfer.[7,8] In fact the corresponding values were 9.0×10^{-6} (**1a**), 9.1×10^{-6} (**1b**) and 2.5×10^{-5} cm^2 s^{-1} (**2**). The diffusion coefficients of **1a** and **1b** were equal, but the diffusion coefficient of **2** was significantly higher.

Conclusions

It was found that the diastereomeric cyclophanes **1a** and **1b** show different electrochemical behaviour during cyclic voltammetry. Compound **1a** exhibited the expected EE-mechanism, but for **1b** the EC-mechanism was observed due to its spatial situation. In **1b** the two six-membered rings of the heterocyclic systems are neighboured in a manner that a chemical reaction between them may occur after the first oxidation step. It is known that biindolizines, which are unsubstituted in the reactive 1- and 1′-positions, show the EC-mechanism, too.[3] In the case of **1a**, **1b** and **2** the 1- and 1′-position are substituted. The EC-mechanism of **1b** must be a result of steric stress. In that way we have found an example of a direct connection between diastereomerism and electrochemical behaviour.

Experimental

Methods

NMR data were recorded with a UNITY plus-500 spectrometer and shifts are in ppm ($SiMe_4$ as internal standard,

J in Hz, coupling constants were taken directly from the obtained spectra or by homodecoupling techniques, respectively). The assignments were carried out by various 2D NMR methods (H,H COSY; HSQC and HMQC) by using indirect detection and gradient techniques. Mass spectra were run on a Hewlett Packard 5985 B (electron impact, 70 eV, direct inlet and FAB-MS). Melting points are uncorrected (Boëtius apparatus). TLC was carried out on plastic plates coated with silica gel 60 F_{254} (5735) (Merck), and flash chromatography on Merck silica gel 60 (7731) (Merck).

Cyclic voltammetry

Cyclic voltammograms were recorded on a Metrohm instrument equipped with a PGSTAT 20 potentiostat. A three electrode system was adopted. The working electrode was a platinum disk of 3 mm diameter, the counter electrode was a platinum wire and the reference electrode assembly was Ag/AgCl/0.1 mol dm^{-3} LiCl–ethanol/fine porosity glass disk/0.1 mol dm^{-3} Bu_4NPF_6–acetonitrile/fine porosity glass disk. The electrolytic solvent was acetonitrile (selectophore quality by Fluka) containing 0.1 mol dm^{-3} Bu_4NPF_6. All measurements were carried out in an argon atmosphere at room temp. The reference electrode had a potential of +0.491 V *vs*. the ferrocene electrode Fc/Fc^+.

Materials

2-[3-(1,3-Dioxolan-2-yl)propyl]pyridine 3. To an ice-cooled mixture of BuLi (4 ml, 10 mmol, 2.5 M in hexane) in 10 ml of tetrahydrofuran (THF) a solution of α-picoline (1 ml, 10 mmol) in 5 ml of THF was added during 10 min. Lithiation was completed after 60 min at the same temperature, and 10 mmol (1.81 g, 1.17 ml) of 2-(2-bromethyl)-1,3-dioxolane in 10 ml of THF were quickly added. The reaction mixture was stirred for an additional 4 h and then quenched by addition of water, washed with water (3 × 10 ml), and dried over $MgSO_4$. After the solvent had been evaporated off, the crude residue was pure enough for further operations. A part of the product was purified by kugelrohr distillation, bp 120 °C at 1.1×10^{-2} mmHg (Found: C, 67.8; H, 7.7; N, 7.1. $C_{11}H_{15}NO_2$ requires C, 68.4; H, 7.8; N, 7.25%); $\delta_H(CDCl_3)$ 8.51 (1 H, ddd, *J* 5.1, 1.9 and 1.1, 6-H), 7.57 (1 H, td, *J* 7.6, 7.6 and 1.9, 4-H), 7.15 (1 H, td, *J* 7.6, 1.9 and 1.1, 3-H), 7.08 (1 H, ddd, *J* 7.6, 5.1 and 1.1, 5-H), 4.88 [1 H, t, *J* 4.7 CH_2–C*H*–$(O)_2$], 3.95 (2 H, m, O–C*H*$_2$–C*H*$_2$–O), 3.84 (2 H, m, O–C*H*$_2$–C*H*$_2$–O), 2.84 (2 H, t, *J* 7.7, C–C*H*–CH_2), 1.87 (1 H, m, CH–C*H*$_2$–CH_2), 1.73 (1 H, m, CH_2–C*H*$_2$–CH_2); $\delta_C(CDCl_3)$ 161.8 (s), 149.2 (d), 136.3 (d), 122.7 (d), 121.0 (d), 104.4 (d), 64.8 (t), 38.0 (t), 33.4 (t) and 24.2 (t); M(NH_3 CI) *m*/*z* 194 ([M + H]$^+$, 100%), 150 (54), 132 (8), 120 (9), 91 (21) and 72 (13).

1-[2-(1,3-Dioxolan-2-yl)ethyl]2-phenylindolizine 4. A stirred mixture of the crude pyridines (*ca*. 8 mmol) in acetone (30 ml) was refluxed and an acetone (10 ml) solution of the ω-bromacetophenone (2 g, 10 mmol) was added. The mixture was refluxed for additional 6 h. After removing the solvent with a rotary evaporator, the pyridinium bromide was obtained as a semisolid compound. The crude bromide was suspended in 15 ml of water containing $NaHCO_3$ (4.2 g, 50 mmol) and refluxed with stirring for 3 h. The reaction mixture was cooled and extracted with toluene (3 × 30 ml). The organic layer was washed with water (3 × 10 ml), dried over $MgSO_4$, and concentrated under reduced pressure. A first purification was carried out by flash chromatography (toluene). The oily residue was pure enough for further operations. A part of the product was purified for analysis by kugelrohr distillation, bp 190 °C at 2×10^{-2} mm Hg; $\delta_H[(CD_3)_2SO]$‡ 8.16 (1 H, td, *J* 6.9, 1.1, 5-H), 7.64 (1 H, s, 3-H), 7.50 (2 H, m, Ph-2-H and Ph-6-H), 7.43 (2 H, m, Ph-3-H and Ph-5-H), 7.30 (1 H, tt, *J* 7.3, 1.5, Ph-4-H), 7.38 (1 H, td, *J* 9.0, 1.1, 8-H), 6.65 (1 H, ddd, *J* 9.0, 7.1 and 1.1, 7-H), 6.50 (1 H, td, *J* 7.1, 6.9 and 1.1, 6-H), 4.76 [1 H, t, *J* 4.8, CH_2–C*H*$_2$–$(O)_2$], 3.86 (2 H, m, O–C*H*$_2$–C*H*$_2$–O), 3.75 (2 H, m O–C*H*$_2$–C*H*$_2$–O), 2.91 (2 H, m, C–C*H*$_2$–CH_2), 1.76 (2 H, m, CH–C*H*$_2$–CH_2); $\delta_C[(CD_3)_2SO]$‡ 135.64 (s, Ph-C-1), 130.12 (s, C-9), 128.54 (d, Ph-C-2 and Ph-C-6), 128.17 (d, Ph-C-3 and Ph-C-5), 127.80 (s, C-2), 126.28 (d, Ph-C-4), 125.35 (d, C-5), 116.96 (d, C-8), 116.16 (d, C-7), 110.64 (d, C-3), 110.05 (d, C-6), 108.90 (s, C-1), 103.15 [d, CH_2-*C*H-$(O)_2$], 64.22 (t, O–*C*H$_2$–CH_2O), 35.00 (t, C–*C*H$_2$–CH_2), 18.31 (t, CH–*C*H$_2$–CH_2); M (NH_3 CI) *m*/*z* 293 (M$^+$, 86%), 218 (7), 206 (100), 193 (100), 105 (19). $C_{19}H_{19}NO_2$ requires 293.

1,1′-Bis[2-(1,3-dioxolan-2-yl)ethyl]-2,2′-diphenyl-3,3′-biindolizine 2. $K_3[Fe(CN)_6]$ (3.29 g, 10 mmol) was added to a solution of $NEt_3 \cdot x HClO_4$ (0.5 g, 2.5 mmol) in 100 ml of ethanol. The suspension was stirred for 10 min and then treated with a solution of *ca*. 6 mmol of indolizine in 50 ml of toluene. After stirring at room temp. for 20 h the solvent was evaporated under reduced pressure. The mixture was taken up with toluene and water. The organic layer was separated and dried ($MgSO_4$), and the solvent was evaporated under reduced pressure. Purification by flash chromatography (toluene) yielded the pure biindolizine as a brown oil. Yellow crystals were obtained by storage in a refrigerator. Yield 0.96 g (about 55%), mp 152–154 °C; (Found C, 77.71; H, 6.29; N, 4.31. $C_{38}H_{36}N_2O_4$ requires C, 78.06; H, 6.21; N, 4.79%); $\delta_H[(CD_3)_2SO]$‡ 7.49 (2 H, td, *J* 8.9, 1.2 and 0.9, 5-H), 7.24 (2 H, td, *J* 6.9, 6.4 and 1.2, 8-H), 7.17 (6 H, m, Ph-3-H, Ph-4-H and Ph-5-H), 6.93 (4 H, m, Ph-2-H and Ph-6-H), 6.73 (2 H, td, *J* 8.9, 6.4 and 0.9, 6-H), 6.43 (2 H, ddd, *J* 6.9, 6.4 and 1.2, 7-H), 4.71 [2 H, t, *J* 4.8, CH_2–C*H*–$(O)_2$], 3.84 (4 H, m, O–C*H*$_2$–C*H*$_2$–O), 3.72 (4 H, O–C*H*$_2$–C*H*$_2$–O), 2.82 (4 H, m, C–C*H*$_2$–CH_2), 1.72 (4 H, m, CH–C*H*$_2$–CH_2); $\delta_C[(CD_3)_2SO]$‡ 134.89 (s, Ph-C-1), 130.46 (s, C-9), 130.18 (s, C-3), 128.60 (d, Ph-C-3 and Ph-C-5), 127.86 (d, Ph-C-2 and Ph-C-6), 126.32 (d, Ph-C-4), 122.46 (d, C-8), 117.12 (d, C-5), 117.07 (d, C-6), 110.71 (d, C-7), 110.34 (s, C-1), 110.14 (s, C-2), 102.97 [d, CH_2–*C*H–$(O)_2$], 64.06 (t, O–*C*H$_2$–*C*H$_2$–O), 34.91 (t, C–*C*H$_2$–CH_2), 18.26 (t, CH–*C*H$_2$–CH_2); M (FAB) *m*/*z* 584 (M$^+$, 100%), 540 (4) and 497 (25).

‡ 2D NMR spectroscopy revealed an exact assignment of all H and C atoms. In the dimerization product **2** we observe not only a strong chemical shift of H and C atoms in the direct neighbourhood of the substitution position C-3, but also a remarkable shift of all the other signals of the indolizine system and a change in signal order. The 2D NMR spectra are available as supplementary material (Suppl. No. 57197, 3 pp.) from the British Library. For details of the Supplementary Publications Scheme, see 'Instructions for Authors', *J. Chem. Soc., Perkin Trans. 2*, 1997, Issue 1.

References

1 H. Sonnenschein, T. Kreher, E. Gründemann, R.-P. Krüger, A. Kunath and V. Zabel, *J. Org. Chem.*, 1996, **61**, 710.
2 S. Hünig and F. Linhart, *Liebigs Ann. Chem.*, 1976, 317.
3 L. Cardellini, P. Carloni, L. Greci, G. Tosi, R. Andruzzi, G. Marrosu and A. Trazza, *J. Chem. Soc., Perkin Trans. 2*, 1990, 2117; G. Gambini, P. Carloni, S. Zamponi, P. Conti, L. Greci and R. Marass, *J. Chem. Res.* (*M*), 1995, 135.
4 S. Hünig and H. Sonnenschein, *J. Prakt. Chem.*, 1994, **336**, 38.
5 T. Kreher, H. Sonnenschein, L. Schmidt and S. Hünig, *Liebigs Ann. Chem.*, 1994, 1173.
6 S. Hünig, *Liebigs Ann. Chem.*, 1964, **676**, 32.
7 D. K. Gosser, *Cyclic voltammetry*, VCH, New York, 1993.
8 A. J. Bard and L. R. Faulkner, *Electrochemical methods*, Wiley, New York, 1980.
9 D. S. Polcyn and I. Shain, *Anal. Chem.*, 1966, **38**, 370.

Paper 6/03333D
Received 13*th May* 1996
Accepted 23*rd October* 1996